VOLUME 32 NUMBER 12

ACCOUNTS of CHEMICAL RESEARCH®

DECEMBER 1999

Origin of Methyl Internal Rotation Barriers

LIONEL GOODMAN* AND VOJISLAVA POPHRISTIC

Wright and Rieman Chemistry Laboratories, Rutgers University, New Brunswick, New Jersey 08903

FRANK WEINHOLD

Chemistry Department, University of Wisconsin, Madison, Wisconsin 53706

Received April 28, 1999

1. Introduction

Barriers to internal rotation about single bonds are among the major factors controlling the conformations of molecules. The interest for resolving basic physical questions relating to internal rotation extends into our thinking about large-amplitude vibrations in biologically important systems, since internal rotation determines some crucial characteristics of the structure, and consequently of the function of carbohydrates, nucleic acids, and proteins.

Possible explanations for the electronic origin of these barriers have been formulated in terms of steric repulsions,[1] electrostatic models,[2] hyperconjugation,[3] and other concepts,[3,4] but the nature of barrier forces has remained controversial after more than 60 years of experimental and theoretical study. Enigmas regarding the torsional potential, even for ethane, remain unresolved, and the underlying cause for the barrier in this basic methyl rotor molecule is still being debated. Thus, barrier origins have, to this day, remained the Bermuda Triangle of electronic structural theory:

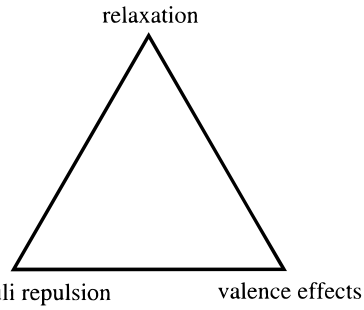

A number of attempts to explain barriers have been made by considering one or two of these factors separately, but only recently has the effect of relaxation been comprehensively considered.[5−8] In this Account, we bring together some recent ideas about barriers, which stem from the *interaction* of Pauli repulsion and valence forces with the relaxation factor. We address questions of barrier origins in three benchmark methyl molecules: ethane, methanol, and dimethyl ether. Our theme is that understanding the barriers in these molecules requires appreciation of how the energy−relaxation connection varies from one case to another.

2. What Is Internal Rotation?

Considerable confusion has resulted from the lack of a unique description of internal rotation. Fully relaxed rotation is defined as a sequence of values in one dihedral angle of a methyl group (the "torsional angle", τ), followed by optimization of all other structural parameters. This adiabatic, minimum energy path for internal rotation is not a pure rotation; it involves skeletal bond expansions and contractions as well as angle changes.[9] Rigid rotation freezes the methyl group and all skeletal internal degrees of freedom. In terms of this latter description, methyl torsion has local mode properties; i.e., it is free of coupling to normal vibrations.

Lionel Goodman studied theoretical chemistry with Harrison Schull and experimental spectroscopy with Michael Kasha. He has held Guggenheim and NSF Senior Fellowships and has been visiting Professor at the Sorbonne and at Stockholm. He particularly enjoys boating on rivers through the French countryside.

Vojislava Torbica Pophristic was brought up in Belgrade, Serbia, Yugoslavia, and studied physical chemistry at the University of Belgrade, graduating Magna cum Lauda. She is presently Bevier Fellow at Rutgers University, where she is finalizing her Ph.D. dissertation on origin of internal rotation barriers with Lionel Goodman.

Frank Weinhold was born in western Nebraska and studied chemistry at Boulder, Freiburg, Harvard (with E. B. Wilson, Jr.), and Oxford (with C. A. Coulson). He came to Wisconsin in 1976 and now concentrates on the nature of water, often in proximity to scenic geological features along the state's principal river.

10.1021/ar990069f CCC: $18.00
Published on Web 11/04/1999

However, most methyl molecules have unequal methyl bond lengths and angles for the equilibrium conformation, not allowing rigid rotation to generate a three-fold-symmetric potential.[10,11] One remedy has been to regard the methyl group as a rigid symmetric rotor with local C_{3v} symmetry. Another dilemma is that, although the "reference" hydrogen rotation angle can be fixed in fully relaxed rotation, the other two methyl hydrogens do not undergo the same torsional displacement. One way to avoid this ambiguity is to define τ as the average of the three hydrogen atom rotations from the equilibrium geometry.[10]

The reaction path approach treats internal rotation as a reaction leading from one rotamer to another in terms of a unique rotation coordinate.[12,13] Coupling between the rotation and the remaining degrees of freedom is included by the reaction path Hamiltonian. Since in this Account we are primarily concerned with barriers, not potential shapes (i.e., $\delta E/\delta t$ and $\delta^2 E/\delta \tau^2$), the torsional potential is regarded as merely a useful path connecting the stationary points. It is the powerful effect of skeletal motions on barrier mechanisms that is the subject of this Account.

3. Comparison of Theory and Experiment

Ab initio molecular orbital calculations have increasingly become the method of choice for obtaining information about barriers. However, ab initio barriers cannot be directly compared to experimental barriers. The calculated ΔE_{total} values represent the difference in energy between the bottom of the equilibrium state potential well and that for the rotated metastable state. Classical experiments, determining rotational barriers, largely utilized low-temperature heat capacity measurements and splittings of microwave transitions.[14] Barriers obtained in this fashion require a correction for the zero-point energy difference between the equilibrium and metastable top-of-barrier states because the vibrational modes are not identical in the two states.[15] Other approaches involve measurement of torsional fundamental and overtone energy levels by far-infrared and fluorescence spectroscopy, and hot band analysis of visible and ultraviolet electronic spectra. These measurements allow torsional potentials to be obtained by fitting the measured energy levels to a rigid rotor Schrödinger equation.[14]

The increased clarity and narrow lines that are available through supersonic jet-cooled spectroscopy have made this technique a powerful tool for probing methyl torsional modes. Recent torsional region Rydberg state[16] and zero kinetic energy jet experiments on radical cations[17,18] have allowed barriers to be obtained for states which have electron distributions very different from those of the ground state. Insight into torsional barrier origins can then be obtained by comparison of these potential energy surfaces with the ground state.

All of these approaches suffer from the problem that fitting experimental transitions by an effective one-dimensional potential involving a single torsional angle cannot correspond exactly to a multidimensional potential

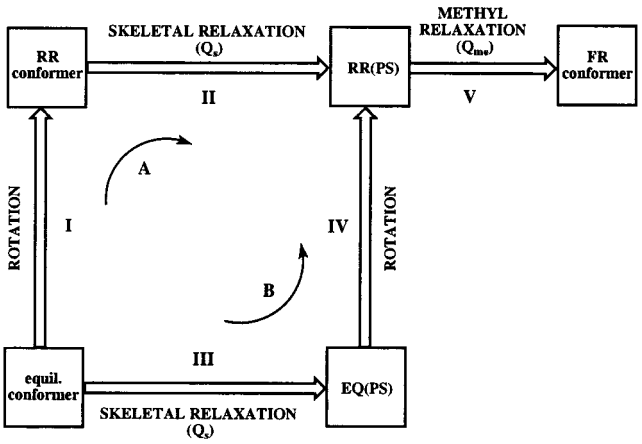

FIGURE 1. Alternate internal rotation paths to the fully relaxed (FR) metastable conformer. In path A (steps I and II), step I, rigid rotation (RR) from the equilibrium conformer is followed by relaxation along the *s*th skeletal coordinate {Q_s (step II)}. Path B (steps III and IV) relaxes Q_s in the equilibrium conformer (step III) to its optimized value {the "prepared" state, EQ(PS)}, followed by rotation from EQ-(PS) (step IV). Step V relaxes the methyl coordinates, Q_{me}, to their fully relaxed values.

calculated by electronic structure methods. In contrast, ab initio barriers are well-defined quantities representing the difference between stationary points on a full multi-dimensional potential energy surface. Their ability to provide an understanding of such diverse problems as conformational analysis and reaction dynamics has made ab initio-calculated torsional barriers a powerful tool.

4. Flexing Analysis of Internal Rotation Energetics

We turn to the principal theme of this Account, flexing dependence of steric repulsions and valence interactions. Our approach utilizes the internal rotation paths defined in Figure 1 to clarify how relaxations accompanying torsion affect interactions contributing to the barrier energy. Dissection of fully relaxed rotation into individual bond length and angle displacements separates the skeletal and methyl folding relaxations from the torsional rotation of the methyl group.

It is possible to analyze the barrier using an energy decomposition expressed in terms of kinetic and electrostatic potential energy (electron−nuclear attraction, electron and nuclear repulsion) changes.[19] However, inherent in the electrostatic categories (but effectively hidden by this approach) are interactions (e.g., hyperconjugation and steric effects) that would be meaningful to the chemical community. Thus, this decomposition did not lead to the expected understanding of barrier mechanisms. Another approach is to explicitly partition the energy into more understandable interactions: structural (ΔE_{struct}), hyperconjugative (ΔE_{deloc}), and steric repulsion (ΔE_{steric}) changes,[5,20]

$$\Delta E_{total} = \Delta E_{steric} + \Delta E_{struct} + \Delta E_{deloc} \qquad (1)$$

The term "steric repulsion" is taken to refer to the purely quantal effect of electronic exchange antisymmetry

(as opposed to Coulombic repulsion of particles of like charge, a classical effect). It arises as a consequence of the Pauli principle requirement that the *N*-electron wave function be antisymmetric with respect to interchange of pairs of electrons. In effect, wave function antisymmetry provides the "quantum pressure" that resists crowding too many electrons into the same spatial region. As pointed out by Weisskopf,[21] this steric pressure can be pictured in terms of the increased oscillatory and nodal features needed to preserve the mutual orthogonality of doubly occupied orbitals that are forced into the same spatial region (such oscillations corresponding to higher wave function curvature and increased kinetic energy). Because the Pauli exchange repulsions vary exponentially with distance, they rapidly dominate other interactions, such as the Coulombic repulsion of nuclei, which varies only as $1/R$. Steric exchange forces underlie the "hardness" of macroscopic matter (e.g., the ability of a mountain base to withstand the enormous gravitational overburden without plastic deformation) as well as numerous molecular-level phenomena. The Weisskopf formulation of steric repulsions can be evaluated in terms of the energy difference between filled natural bond orbitals (NBOs) and the corresponding nonorthogonal "pre-NBOs" (PNBOs),[22] which differ from NBOs only in omission of the orthogonalization step. Steric exchange repulsions inherently involve a collective response of the entire *N*-electron system, denoted as "total exchange repulsion" to discriminate this simultaneous all-electron effect from the pairwise exchange energy obtained by summing independent pair interactions between local bond orbitals. It is precisely because exchange repulsions involve all electrons simultaneously that appreciating their relaxation dependence is essential to understanding the repulsions themselves.

The structural energy is determined by a Hartree product of doubly occupied PNBOs comprising the core, lone pairs, and localized bonds of the "Lewis" structure and consequently contains many of the electrostatic interactions, such as nuclear and electron repulsion. Its usefulness is that its change directly relates to bond weakenings (or strengthenings) and lone-pair reorganizations. The delocalization energy change (ΔE_{deloc}) represents hyperconjugative (charge-transfer, CT) interaction effects, and we will use these terms interchangeably. This interaction depends on the relative orientation of donor and acceptor orbitals and consequently leads to stereoelectronic effects.[3,23]

Thus, all three terms in eq 1 can be expected to relate to the details of the internal rotation coordinate. The question that needs to be answered is the following: How does the interplay of ΔE_{struct}, ΔE_{deloc}, and ΔE_{steric} stereoelectronic dependencies affect the barrier?

Our discussion utilizes the NBO scheme originated by Foster and Weinhold.[24] The calculation algorithms have been given by us.[5,25] Several ab initio theory levels have been employed to ensure that our conclusions are stable to both changes in basis set and inclusion of electron correlation.

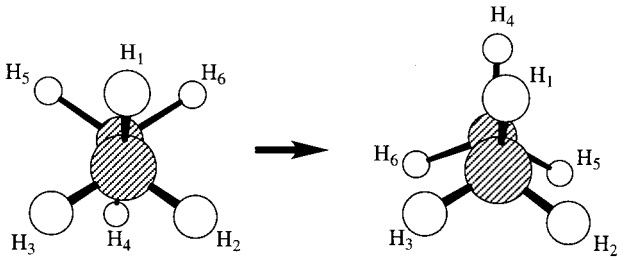

FIGURE 2. Ethane internal rotation. The C_aH_1/C_bH_5 bond pair is classified *gauche* in either conformer, and C_aH_1/C_bH_4 *anti* and *syn* in the staggered (S) and eclipsed (E) conformers, respectively.

Table 1. Internal Rotation Barriers (kcal/mol)[a]

level	ethane	methanol	DME
HF	3.04	1.09	4.26
MP2	2.90	1.12	4.72
MP4(SDTQ)	2.81	1.12	4.60
CISD	2.79	1.09	4.55
CCSD(T)	2.79	1.09	4.57

[a] Basis set 6-311G(3df,2p). Geometry optimization MP2.

5. Ethane

Ethane internal rotation (Figure 2), with its special place as a prototype molecule for methyl rotation about a single bond, has attracted continuing interest. Ab initio calculations have been quite successful in simulating the 2.9 kcal/mol barrier (Table 1). Probably the first detailed elucidation for the barrier, by Sovers, Kern, Pitzer, and Karplus[1] in 1968, involved increased steric repulsion between C−H bonds in the top-of-barrier eclipsed (E) conformer due to the C_aH_1 and C_bH_4 hydrogens' closer approach (see Figure 2).[26] But post-1990 studies of Pauli repulsion have challenged this view. Bader et al.'s atomic basin considerations,[4] Badenhoop and Weinhold's NBO calculations,[23] and the recent large basis set relaxation studies of Goodman and Gu[7] conclude that the *total* exchange repulsion (unlike the C−H/C−H *pairwise* repulsions) destabilizes the S conformer more than the E conformer. The outcome is that the overall exchange repulsion does not form the barrier, even though *anti/syn* and *gauche* H−H distances respectively decrease and increase in the E conformer. Another counterintuitive conclusion of the large basis set studies[7] is that *anti/syn* C−H pair repulsions actually are antibarrier and *gauche* repulsions barrier forming, opposite to the barrier-forming *anti-syn* C−H pairwise interactions found in previous ethane steric considerations.

Other principal explanations have invoked hyperconjugative charge-transfer interactions between the six methyl σ_{CH} occupied orbitals and associated σ^*_{CH} antibonding unfilled orbitals preferentially stabilizing the S conformer (primarily due to stronger *anti* $\sigma_{CH}-\sigma^*_{CH}$ interactions than for *syn*);[3,22] and Coulombic repulsion between methyl C−H bonds, resulting from bond distance reduction in the E conformer.[2] Mulliken,[27] as early as 1939, conjectured that hyperconjugation plays an important role in the internal rotation potential of ethane-like molecules. However, Mulliken's initial estimate of these effects was very crude, seeming to suggest that they were too small to account for observed barriers, and the idea was largely

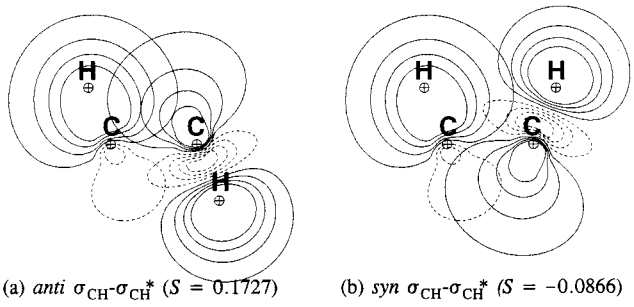

(a) *anti* σ_{CH}-σ^*_{CH} (S = 0.1727) (b) *syn* σ_{CH}-σ^*_{CH} (S = −0.0866)

FIGURE 3. Leading $\sigma_{CH}-\sigma^*_{CH}$ hyperconjugative donor−acceptor interactions in the staggered (a) and eclipsed (b) conformers of ethane. Calculation level B3LYP/6-311++G(d,p).

forgotten until the semiempirical MO studies of Brunck and Weinhold[20] in the 1970s.

Another tack was taken by Goodman, Gu, and Pophristic.[5] Although the rigid rotation barrier (3.2 kcal/mol)[9] is only slightly altered (<5%) from the fully relaxed one, they approached the ethane barrier question from the viewpoint that the internal rotation coordinate is very impure (see Section 2). As a consequence, the barrier mechanism should reflect those energetic changes that are engendered by C−C expansion and methyl folding attendant to the torsion. Relaxation leaves the delocalization energy essentially intact but has powerful consequences to the exchange repulsion and structural energy terms in eq 1.[5]

The dependence of ΔE_{deloc} on the *shapes* of vicinal σ_{CH},σ^*_{CH} bond orbitals in the *anti* and *syn* arrangements of staggered and eclipsed conformers was revealed by Brunck and Weinhold's early semiempirical study and is confirmed by our more elaborate ab initio ones (Figure 3). It is clear that the $\sigma_{CH}-\sigma_{CH^*}$ donor−acceptor interactions are sharply reduced in the *syn* arrangement compared to *anti*, due to unfavorable cancellation in the latter case as the nodal plane of the CH antibond orbital cuts through the main lobe of the CH bond orbital. This visual estimate is confirmed by the overlap integral magnitude, S (Figure 3), which strongly favor larger hyperconjugative stabilizations in the staggered conformer. As can be seen from Table 2, ΔE_{deloc} for *geminal* bond/antibond CTs is much smaller than for vicinal charge-transfers between the methyl groups. The difference arises because geminal interactions involve no direct coupling between groups on opposite ends of the rotor axis. Table 2 provides further insight into the vicinal interactions by decomposing these into 6 *anti/syn* charge-transfers and 12 *gauche/gauche* ones. ΔE_{deloc} for the *anti/syn* vicinal interactions strongly dominates, providing the principal reason for the preferential hyperconjugative stabilization of the S conformer.

Rotation causes lengthening of the ethane C−C bond by 0.014 Å (Table 3). Many studies have established that the barrier is almost independent of this large structural change, the small correction leading to the delusion that the barrier can be understood in terms of rigid rotation. However, the recent demonstration by Goodman and Gu[7] that the exchange repulsion is strongly sensitive to the C−C bond expansion has far-reaching consequences for understanding the ethane barrier. Figures 4 and 5 show the torsional angle dependence of the barrier energy

Table 2. Ethane Natural Bond Orbital Bond−Antibond (Charge-Transfer) Interactions (kcal/mol)[a]

interaction pair	E_{deloc} (S)	E_{deloc} (E)	ΔE_{deloc}[c]
vicinal interactions			
C_a-H_1/C_b-H_4* (*anti/syn*, 1 pair)[b]	−3.41	−1.44	1.97
C_a-H_1/C_b-H_5* (*gauche/gauche*, 1 pair)[b]	−0.38	−0.84	−0.46
C_a-H_1/C_b-H_4* (*anti/syn*, 6 pairs)[b]	−20.46	−8.46	11.82
C_a-H_1/C_b-H_5* (*gauche/gauche*, 12 pairs)[b]	−4.56	−10.08	−5.52
all 18 pairs	−25.02	−18.72	6.30
geminal interactions			
C_a-C_b/C_a-H_1* (6 pairs)	−2.88	−2.58	0.30
C_a-H_1/C_a-C_b* (6 pairs)	−0.78	−0.60	0.18
C_a-H_1/C_a-H_2* (12 pairs)	−1.08	−1.32	−0.24
all 24 pairs	−4.74	−4.50	0.24
total	−29.76	−23.22	6.54

[a] All calculations at HF/6-311G(3df,3pd) basis. [b] *Syn*, *anti*, and *gauche* designations are defined in Figure 2. [c] $\Delta E_{deloc} = E_{deloc}(E) - E_{deloc}(S)$.

Table 3. Optimized Ethane Geometries (Bond Lengths in Angstroms, Angles in Degrees)[a]

conformer	C−C	C−H	∠HCH	H_1- -H_4
staggered	1.5233	1.0888	107.6	3.0768
eclipsed	1.5369	1.0878	107.1	2.3419
Δ	0.0136	−0.001	−0.5	−0.7349

[a] MP2/6-311G(3df,2p) optimization.

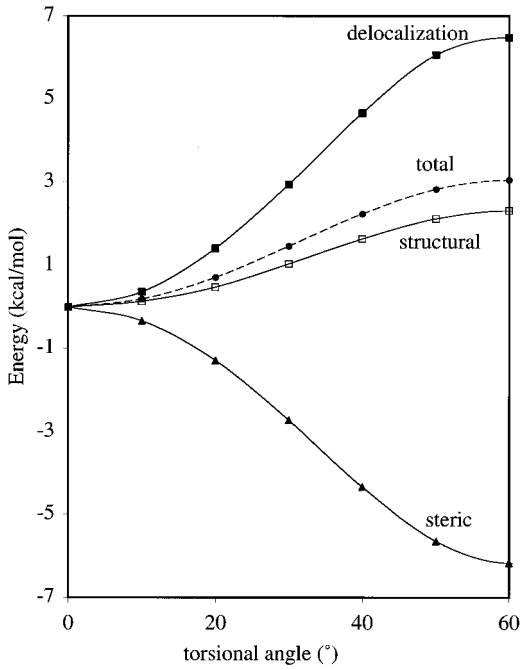

FIGURE 4. Rotational dependence of the energy components (solid curves) of the fully relaxed ethane internal rotation energy (dashed curve) as defined in eq 1. Basis set 6-311G(3df,3pd). Note the strong anticorrelation of the delocalization and steric contributions to the total energy.

decomposition terms for fully relaxed and rigid rotation, respectively. There are several conclusions. Comparison of these two figures shows that the effect of relaxation on the individual energy components is much larger than the effect on the total energy. ΔE_{deloc} (~7 kcal/mol) is the largest barrier-forming term, even exceeding Reed and

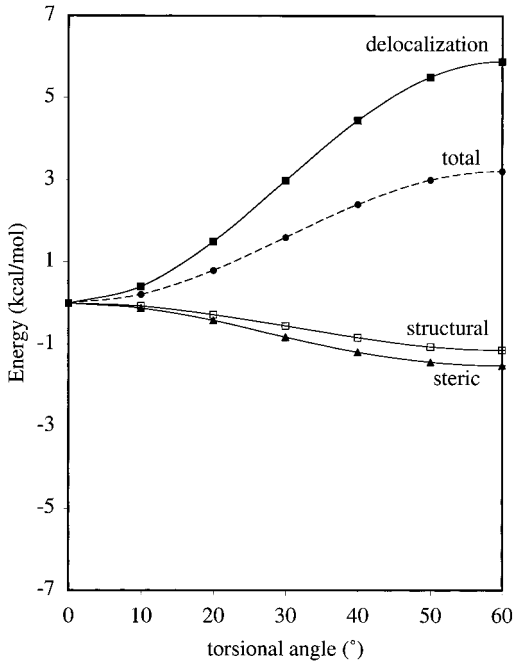

FIGURE 5. Rotational dependence of the energy components (solid curves) of the ethane rigid rotation energy (dashed curve), as defined in eq 1. Basis set 6-311G(3df,3pd).

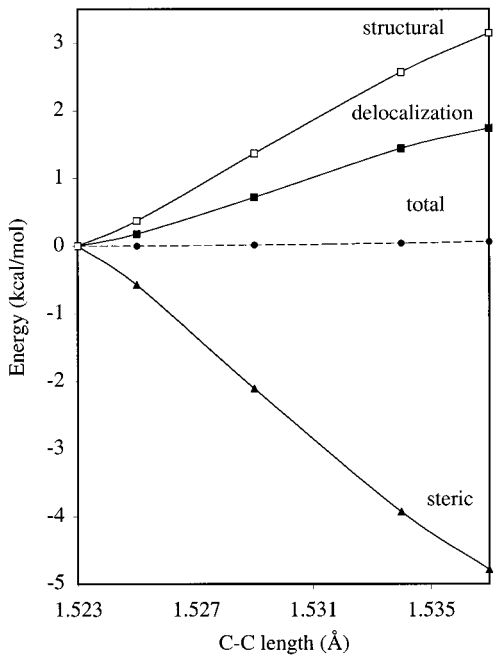

FIGURE 6. Effect of ethane C−C bond relaxation (step III of Figure 1, $Q_s = \Delta R_{C-C}$) on the energy components of eq 1. Designations are the same as in Figures 4 and 5. Note that step III has no internal rotation.

Weinhold's (4.5 kcal/mol) earlier conclusion.[3] *However, as shown in Figure 4, it is largely canceled by the opposite sign steric exchange term*. The calculated (and somewhat basis set dependent) magnitude of ΔE_{struct} ranges from 2.4 to 3.2 kcal/mol. The most important conclusion is that *it is not possible to explain the 2.9 kcal/mol barrier without taking into account the relaxation dependence of all three terms:* ΔE_{struct}, ΔE_{deloc}, and ΔE_{steric}. There is a second conspicuous conclusion: the torsional angle dependence of ΔE_{struct} closely simulates ΔE_{total}.

It is instructive to examine the flexing dependencies of the energy terms in eq 1, using the internal rotation paths defined in Figure 1 to elucidate how the skeletal and methyl relaxations that accompany torsion affect the individual barrier energetics. Ethane is particularly simple in that there are only two relaxations: C−C expansion ($Q_s = \Delta R_{C-C}$) and methyl folding involving both HCH angles and C−H bond lengths ($Q_{me} = \Delta CH_3$). We start with rigid rotation (step I in Figure 1); i.e., the torsional dihedral angle in the equilibrium conformer is rotated, freezing all bond angles and bond lengths. Figure 5 demonstrates that the barrier-forming ΔE_{struct} that accompanied rotation to the fully relaxed transition state reverses sign and consequently is actually antibarrier for the skeletally frozen rotation defined by step I! On the other hand, freezing the skeletal relaxations causes only a modest decrease in ΔE_{deloc}. Figure 5 also demonstrates the great sensitivity of the ethane steric repulsions to skeletal flexing. Nearly 80% of the antibarrier total exchange repulsion change accompanying fully relaxed rotation vanishes for the skeletally frozen rotation defined by step I!

The key to understanding these results is obtained by considering step III. This allows the effect of the most important relaxation, C−C expansion, to be isolated from rotation effects by expanding R_{C-C} in the *equilibrium* conformer to its length in the relaxed rotated conformer, 1.537 Å (EQ(PS) in Figure 1). Figure 6 shows the dependence of the barrier energy decomposition terms on the R_{C-C} expansion. Comparison of the exchange repulsion change that takes place on going to this staggered conformer "prepared state" to the changes induced by fully relaxed rotation displayed in Figure 4 shows that *the total exchange repulsion change for C−C bond expansion in the equilibrium conformer mimics the behavior for fully relaxed rotation*. We emphasize that step III has no internal rotation! The effect of introducing the C−C relaxation in the top-of-barrier eclipsed conformer (step II in Figure 1) is similar to step III. The effect on ΔE_{deloc} is less severe, but still significant. The sum of energy changes for each of the components of ΔE_{total} produced by steps I + II approximates the barrier for fully relaxed rotation; i.e., the energy changes for the remaining methyl relaxation step (V) are minor.

Any understanding of the ethane barrier requires a cause for the C−C expansion accompanying rotation, given the vital role that the expansion plays in the barrier mechanism. On first consideration, it seems likely that steric repulsion is somehow involved since C−C expansion strongly affects ΔE_{steric}. Figure 7 compares PNBO and NBO calculations of the total energy vs C−C bond length for both staggered and eclipsed conformers. The point of this comparison is that the PNBO potential minima represent conformer geometries when exchange repulsions are absent and the NBO minima when exchange repulsions are included. The minima demonstrate that the C−C bond lengths (for both S and E conformers) are shortened (as expected) when the exchange repulsions are removed. But, the inset in Figure 7 provides needed insight into the

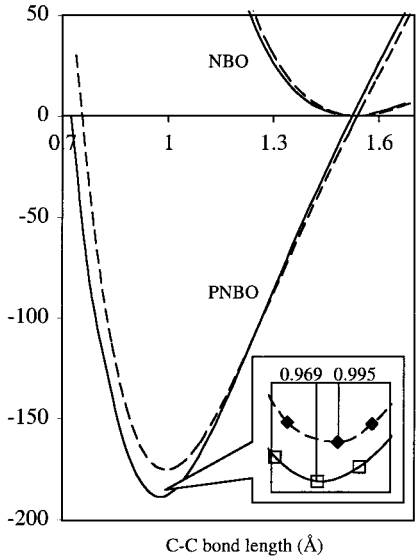

FIGURE 7. Ethane PNBO/NBO HF/6-311G(3df,3pd) energy dependencies on C−C bond length. Solid curves, staggered; dashed curves, eclipsed conformers. Inset focuses on the PNBO minima.

connection between internal rotation and the exchange repulsion effect on the C−C bond length. The S conformer PNBO (exchange repulsion absent) minimum energy bond length is *lengthened* from 0.969 to 0.995 Å in E.

Moreover, comparison of the NBO and PNBO minima shows that the effect of including the exchange repulsion is to lengthen the C−C bond by 0.012 Å *less* in the eclipsed conformer than in the staggered one! This seemingly counterintuitive result—exchange repulsion in the E conformer (having nearby C−H bonds) causing a smaller C−C length increase than in the S conformer (where they are further apart)—is consistent with the *total* exchange repulsion preferential destabilization of the S conformer. The implication is that exchange repulsion is not an important cause for the rotation-induced C−C bond expansion.

The delocalization effect on C−C bond lengthening is revealed by systematic removal of charge-transfer interactions by deletion of appropriate Fock matrix elements between C−H bonds and antibonds, followed by geometry optimizations. All of the deletion-optimized S and E geometries have larger C−C bond lengths than those without deletion, showing that charge-transfer interactions play an important role in controlling the overall ethane geometry. However, R_{C-C} is *shortened* (by >0.01 Å) in the eclipsed conformer from that in the staggered one when the *anti* and *syn* matrix elements *alone* are deleted for all basis sets studied. Thus, their inclusion does the inverse, *increasing* R_{C-C}. Deletion of the *gauche* matrix elements alone does the opposite. Finally, deletion of all 18 C−H interactions decreases R_{C-C} by 0.013 Å. We conclude that it is the larger *anti/syn* charge transfers in the staggered conformation that provide a rationalization for the C−C expansion.

The conclusions are the following: (1) The ethane barrier mechanism cannot be understood without taking into account skeletal relaxation—strikingly demonstrated by structural and steric energy changes for C−C bond expansion in the *equilibrium* conformer mimicking their behaviors for fully relaxed rotation. (2) Charge transfer between vicinal *syn* and *anti* C−H bonds is an important source for the C−C expansion; thus, hyperconjugation plays a vital role in the barrier mechanism.

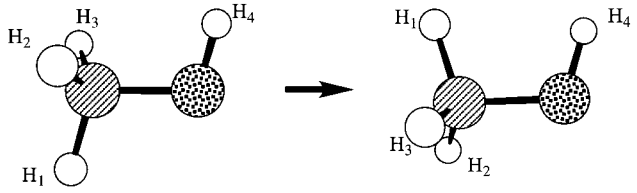

FIGURE 8. Methanol internal rotation.

This ethane barrier mechanism is far from the earlier, on the surface simplistic picture: Pauli repulsion between closely approached C−H bonds in the eclipsed conformer. While steric interactions involving individual bond−bond interactions are useful quantities to calculate and understand, this picture is supplanted by a more subtle complex view involving the energy−relaxation interactions. The outcome is that neglect of relaxation leads to a false intuition about barriers in ethane-like molecules. In subsequent sections, we demonstrate how changing the ethane chemical structure alters the energy−relaxation connection.

6. Methanol

Methanol, CH_3OH, can be regarded as ethane with one methyl group replaced by OH. Calculated equilibrium (S) and 180° rotated (E) structures have C_s symmetry, and the internal rotation barrier, slightly greater than 1 kcal/mol (Table 1), is only about one-third that of ethane. This fact would appear to fit the Pauli repulsion model, since there is one CH−OH eclipsed interaction in methanol's metastable (E) state (CH_1-OH_4 in Figure 8), while in ethane there are three. This view, having steric exchange repulsion controlled by overlap interaction between localized orbitals, was derived from an analysis of methanol with idealized geometry, with no relaxation.[1] Both the *pairwise* exchange repulsion and neglect of relaxation assumptions were shown for ethane (Section 5) to give an incorrect appreciation of the steric repulsion.

Rotation of the methyl group, in contrast to the large (0.014 Å) C−C expansion found for ethane, produces relatively small C−O bond lengthening and O−H bond shortening, shown in Table 4. However, there are two major angle openings: the $H_{ip}CO$ angle and the methyl tilt angle; the other angular changes are less important. The combined rotation-induced relaxations lead to H−H distance changes virtually the same as those for ethane.

The rigid rotation barrier (step I in Figure 1) is calculated to be much higher (i.e., doubled, see Table 5) than the fully relaxed one. This strong barrier reduction caused by relaxation is in marked contrast to the relaxation insensitivity exhibited by the ethane barrier (Section 5). Relaxations responsible for the decrease can be found by examining the barrier energy flexing dependence. Fully

Table 4. Optimized Geometries for Methanol and Dimethyl Ether

	methanol[a]		DME[a]	
	S	E	EE	SS
bond lengths (Å)				
$C_{me}-O$	1.4014	1.4049	1.3903	1.3945
$C_{me}-H_{ip}$	1.0812	1.0858	1.0823	1.0860
$C_{me}-H_{op}$	1.0872	1.0843	1.0896	1.0861
O−H	0.9423	0.9405		
angles (deg)				
C−O−H (C−O−C)[b]	110.5	111.2	113.7	118.6
$H_{ip}-C_{me}-O$	107.1	112.0	107.7	112.2
$H_{op}-C_{me}-O$	111.8	109.5	111.5	109.8
CH_3 tilt[c]	1.7	3.2	3.6	1.5

[a] Geometry optimization: methanol, HF/6-31++G(d,p); DME, HF/6-31G(2d,p). [b] COH, methanol; COC, DME. [c] Defined as deviation of the $C_{me}-O$ bond axis from the normal to the plane defined by the three methyl hydrogens.

Table 5. Methanol Barrier Relaxation[a] Effects (kcal/mol)[b]

relaxation	barrier
rigid rotation	1.99
CO bond lengthening	2.03
∠COH opening	1.97
CH_3 group flexing	1.07
fully relaxed internal rotation	1.02

[a] All relaxation energies refer to rotation with indicated flexing. [b] HF/6-311++G(3df,2p) energy calculation; MP2/6-311G(3df,2p) geometry optimization.

relaxed rotation in methanol can be usefully broken down into four partial relaxations: C−O expansion and O−H shortening, COH angle opening, and methyl group relaxation. Methyl relaxation is a composite relaxation comprising $C-H_{ip}$ bond expansion, $C-H_{op}$ bond shortening, and methyl tilt angle opening (see footnote *c*, Table 4). Table 5 shows the effect of the most important partial relaxations on the barrier energy. This is accomplished by allowing the relevant internal coordinate (Q_i) to assume its fully relaxed top-of-barrier value, while all the other internal coordinates are kept frozen at their equilibrium values (except the dihedral angle defining methyl rotation). Only the methyl group relaxation is found to play an important role, lowering the barrier to approximately the fully relaxed value.

The methanol torsional barrier energy breakdown is shown in Figure 9. Charge-transfer interactions preferentially stabilize the equilibrium conformer, resulting in a barrier-forming ΔE_{deloc}. The exchange repulsion, ΔE_{steric}, is antibarrier and is poorly approximated by the pairwise repulsion (see Table 6). All these results are parallel to those for ethane. However, the structural energy change, ΔE_{struct}, is now the largest barrier-forming term. Furthermore, the largest contribution to ΔE_{struct} is found for the rigid rotation step (Table 6), which accounts for >80% of the fully relaxed value, opposite to the antibarrier rigid rotation behavior in ethane. The dominance and sign of ΔE_{struct} suggest that the structural energy change has its roots in a process present in methanol but absent in ethane−lone pair reorganization.[8]

The large barrier reduction on going from ethane to methanol is attributed to the altered charge-transfer interactions; i.e., in methanol there is a large antibarrier

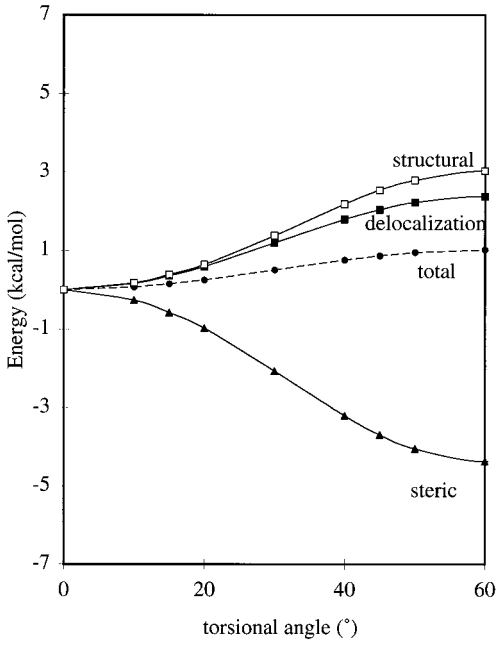

FIGURE 9. Rotational dependence of the energy components (solid curves) of the fully relaxed methanol internal rotation energy (dashed curve) as defined in eq 1. HF/6-311++G(3df,2p) energy calculation; MP2/6-311G(3df,2p) geometry optimization.

Table 6. Principal Methanol Stepwise[a] Energy Decomposition Changes (kcal/mol)[b]

path	step	total	delocalization	structural	total steric	pairwise steric
A	I	1.99	2.60	2.60	−3.21	1.43
	II	0.04	0.42	0.84	−1.22	−0.58
	V	−1.01	−0.64	−0.31	−0.06	−0.82
B[c]	III	0.05	0.45	0.86	−1.26	−0.54
	IV	1.97	2.56	2.58	−3.17	1.39
	V	−1.01	−0.64	−0.31	−0.06	−0.82
fully relaxed		1.02	2.38	3.01	−4.37	0.03

[a] See Figure 1. [b] See footnote *b*, Table 5. [c] CO flexing in Figure 1.

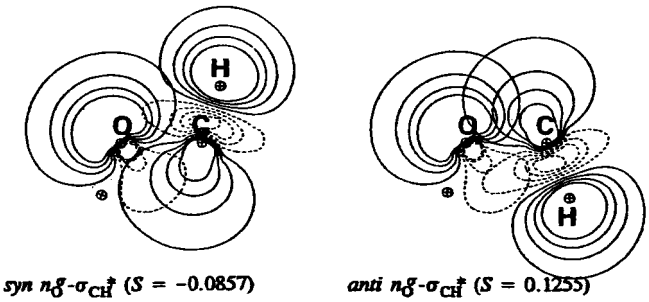

syn n_O-σ_{CH}^* (S = −0.0857) *anti* n_O-σ_{CH}^* (S = 0.1255)

FIGURE 10. Oxygen lone pair (σ)/CH_{ip}* donor−acceptor interactions in *syn* (S, equilibrium) and *anti* (E, top-of-barrier) orientations of methanol. Calculation level B3LYP/6-311++G(d,p).

interaction, lone pair (σ)/CH_1* (Figure 10). The result is that the principal barrier-forming term in ethane, ΔE_{deloc}, becomes much less important in methanol. The energy decomposition also explains the relaxation sensitivity exhibited by the methanol barrier as due to the different relaxation dependencies of ΔE_{deloc}, ΔE_{steric}, and ΔE_{struct} (i.e., steps III and IV of Table 6).

It is instructive to now consider the change of the nuclear−electron attraction component of the electrostatic

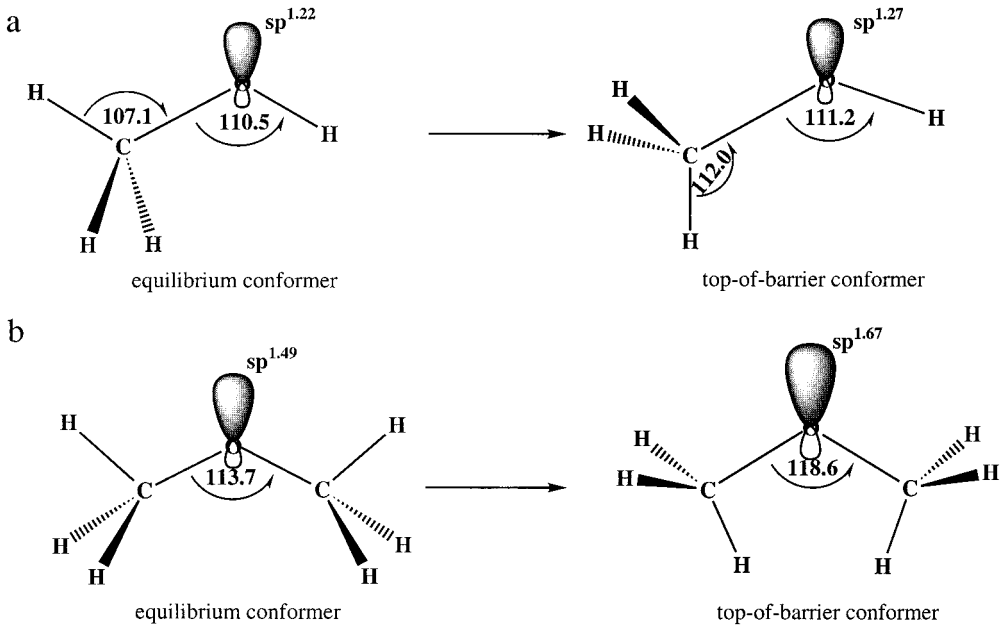

FIGURE 11. Schematic depiction of oxygen σ lone-pair orbital reorganization accompanying internal rotation in methanol (a) and in dimethyl ether (b).

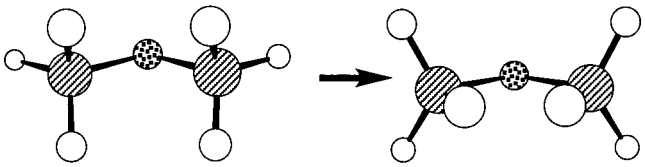

FIGURE 12. DME internal rotation.

potential energy, ΔV_{ne}, which is a constituent of ΔE_{struct}, as indicated earlier. The C_s symmetry allows ΔV_{ne} to be broken down into contributions from A″(π) and A′(σ) orbitals:

$$\Delta V_{ne}\ (\text{kcal/mol}) \qquad A'(\sigma) = 76.2 \qquad A''(\pi) = -17.3.$$

The large barrier-forming σ component provides support for the inference that ΔE_{struct} principally arises from a′ orbital effects, such as the oxygen σ lone-pair reorganization (Figure 11a).[8]

7. Dimethyl Ether

Dimethyl ether (DME), CH_3OCH_3 (Figure 12), can also be regarded as related to ethane, replacing one methyl by the OCH_3 group. Because we are interested in the barrier mechanism rather than the potential surface, we restrict discussion to simultaneous 180° rotation of both methyl groups. DME's special interest is that it has C_{2v} symmetry in both its equilibrium (EE) and simultaneously rotated (SS) structures.[28,29]

The calculated barrier exceeds 4 kcal/mol (Table 1), substantially (>1 kcal/mol) higher than that in ethane and much (>3 kcal/mol) greater than that in methanol. Rotation produces bond length changes similar to the ones found for methanol (Table 4). The major angle flexing is the 5° opening of the COC angle, much larger than the 0.7° COH angular opening in methanol, with other less important angular changes similar to those in methanol.

Table 7. Dimethyl Ether Barrier Relaxation Effects (kcal/mol)[a]

relaxation	barrier
rigid rotation	7.99
∠COC opening[b]	5.58
CO bond lengthening[b]	7.97
CH_3 group flexing[b]	6.18
∠COC opening and CH_3 group flexing[b]	4.26
fully relaxed rotation	4.27

[a] See footnote *b*, Table 5. [b] Simultaneous rotation of both methyl groups plus indicated relaxation(s).

Another important geometry difference is that the combined rotation−relaxation leads to much larger H−H distance changes than in ethane. There is one major relaxation which has no resemblance to those present in either ethane or methanol: the 2° decrease in methyl tilt angle compared to a 1.5° increase in methanol and 0° for ethane.

Table 7 shows that the barrier has similar overall relaxation sensitivity to that found for methanol; i.e., the rigid rotation barrier is much higher (nearly doubled) compared to the fully relaxed one. As for methanol, we break down the relaxed rotation in DME into partial relaxations: in this case, C−O bond expansion, COC angle opening, and methyl group relaxation. Table 7 shows the effect of each of these partial relaxations on the barrier energy, considered individually, and the effect of combining the COC angle opening and methyl flexing. Although both COC angle opening and methyl group relaxation are found to play important roles (that is, they separately substantially decrease the rigid rotation barrier), it is only when these two relaxations are combined that the calculated barrier approaches the fully relaxed value.

Figure 13 shows that, for fully relaxed rotation, the general energy trends are similar to those in methanol: ΔE_{deloc} and ΔE_{struct} are barrier forming, leaving ΔE_{steric} as the only antibarrier component. Comparison of Figure 13

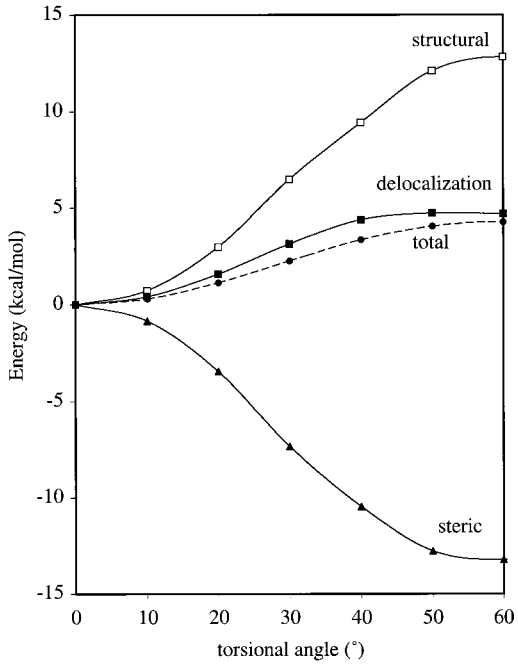

FIGURE 13. Rotational dependence of the energy components (solid curves) of the fully relaxed dimethyl ether antigearing internal rotation energy (dashed curve) as defined in eq 1. HF/6-311++G(3df,2p) energy calculation; MP2/6-311G(3df,2p) geometry optimization.

Table 8. Energetics of the COC Angle Opening in Dimethyl Ether (kcal/mol)[a]

	barrier	ΔE_{steric}	ΔE_{deloc}	ΔE_{struct}
rigid rotation	7.99	10.89	3.61	−6.51
∠COC opening[b]	5.58	−4.99	3.78	6.79
∠COC opening and CH_3 flexing[b]	4.26	−8.44	3.74	8.96
fully relaxed rotation	4.27	−13.23	4.69	12.81

[a] See footnote *b*, Table 5. [b] See footnote *b*, Table 7.

to Figure 9 shows that all are much more strongly so than in methanol. The effect of COC angle opening is shown in Table 8. It is this single partial relaxation that leads to the barrier-forming nature of ΔE_{struct}. For the rigid rotation step (step I in Figure 1), ΔE_{struct} is actually antibarrier. However, there is no single partial relaxation which accounts for the large magnitude (~13 kcal/mol) of the structural energy increase. Table 8 clearly demonstrates the sensitivity of the barrier mechanism to the relaxation details. Even though the barrier is well obtained by combined ∠COC and CH_3 relaxations, the energy decomposition only qualitatively approximates the fully relaxed one.

The large barrier-forming ΔE_{struct} term is largely attributed to reorganization of the lone-pair orbital.[8] The source of the reorganization is the 5° opening of the COC angle, causing the lone-pair p character to increase in going to the barrier top, from $sp^{1.5}$ to $sp^{1.7}$ (Figure 11b). The only other significant (but much smaller) barrier-forming contribution involves the $C-H_{op}$ bond. Consequently, the much higher DME barrier compared to that in methanol is rationalized on the basis of the much increased reorganization of the lone-pair oxygen orbital consequent to opening of the COC angle.

Table 9. Total Electron and Nuclear Repulsion Energy Changes (kcal/mol)[a]

	ethane	methanol	DME
ΔE_{ee}	−96.9	−27.3	−318.3
ΔE_{nn}	−106.2	−33.4	−352.9

[a] Basis set for ethane: see footnote *a*, Table 2. For methanol and DME, basis sets are 6-31++G(d,p) and 6-31G(2d,p), respectively.

8. Concluding Remarks

The thrust of this Account is that mechanisms controlling methyl rotation barriers are correctly revealed only when the *interactions* of the major energetic factors that accompany rotation are taken into account. The importance of obtaining a full complement of barrier energetics when ascribing barrier origins is shown by dissecting the barrier into: Pauli exchange steric repulsion, hyperconjugation, and relaxation energy changes. This unified approach to barrier energetics brings to the forefront the important role of relaxation effects with their consequent bond and lone-pair energy changes in controlling barrier heights.

Two mistaken assumptions that have persistently been made in rationalizing barriers are (i) that steric repulsion increases when two bonds, as a result of rotation, come into closer juxtaposition and (ii) that skeletal relaxation effects do not play an important role in the barrier energetics. Removing either one of these assumptions by itself gave a false understanding of the barrier mechanism; correcting both of these assumptions at the same time yields a quite different understanding.

An example is the contrasting barrier heights in dimethyl ether and methanol. In dimethyl ether, the increased steric contact brought about by simultaneous internal rotation of the methyl groups causes the COC angle to increase. The resulting increased electron-pair repulsion between the oxygen σ lone pair and C−O bonding pairs is relieved by the σ lone pair moving farther away from the oxygen atom, expressed by larger lone-pair p character.[8] It is this final step, the lone-pair reorganization, that *controls* the dimethyl ether barrier height. Steric repulsion then plays only a minor role in determining the *barrier energy*, even though it forces the angle opening (note the cause and effect ambiguity!). Absence of steric contact in methanol removes much of the driving force behind lone-pair reorganization (Figure 11), which, along with decreased charge-transfer interactions in the metastable rotated state, explains methanol's low barrier. In ethane, weakening of the C−C bond represents an important barrier-forming contribution that remains hidden when skeletal relaxation that accompanies methyl rotation is omitted.

We now shift the focus to electron and nuclear repulsions, incorporated in ΔE_{struct} under the umbrella of bond and nonbonding orbital energy changes. Repulsion between bond electron clouds and nuclei that come into closer juxtaposition upon rotation has been looked at in many textbooks as being primarily responsible for the steric effect. But, we emphasize that the steric effect is more appropriately defined as the effect of the application

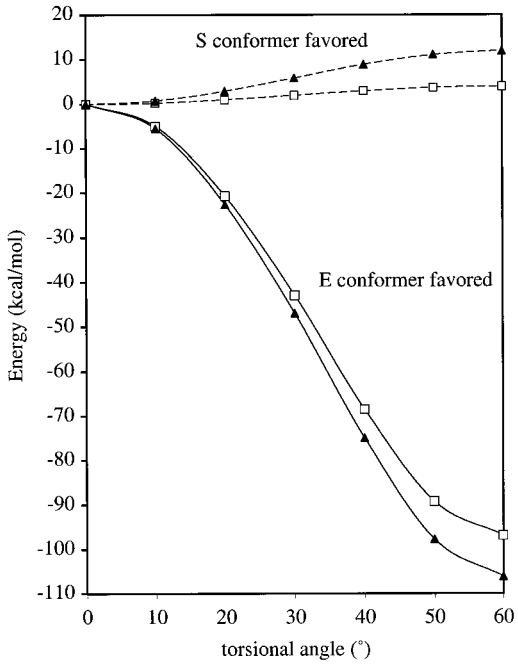

FIGURE 14. Rotational dependence of electron (□) and nuclear (▲) repulsion energies for ethane: solid curve, fully relaxed, and dashed curve, rigid rotation. Basis set 6-311G(3df,3pd).

of an antisymmetrizer to the *N*-electron wave function (see Section 4). Both total electron and nuclear repulsion changes are strongly antibarrier for fully relaxed rotation in the three prototype molecules that we have discussed (Table 9). This result is independent of both basis set composition and whether correlation is included or not.[30] However, examination of the dependencies on the internal rotation path for ethane shows that, without relaxation (step I), the repulsions are barrier forming (Figure 14). If the torsional path includes relaxation, the repulsions change sign from the preferential destabilization of the metastable conformer for the rigid rotation step to preferential destabilization of the equilibrium conformer. Similar results are found for methanol and DME. Thus, while it cannot be said that these repulsions cause the *barrier*, it is fair to state that they play an important (if not vital) role in the *relaxation* mechanism. The striking difference between the rigid and fully relaxed curves in Figure 14 again illustrates the need to consider interdependencies of all of the factors contributing to barrier origins.

Financial support from NSF is gratefully acknowledged.

References

(1) Sovers, O. J.; Kern, C. W.; Pitzer, R. M.; Karplus, M. Bond-Function Analysis of Rotational Barriers: Ethane. *J. Chem. Phys.* **1968**, *49*, 2592−2599.
(2) Wiberg, K. B.; Murcko, M. A. Heats of Reduction of Carbonyl Compounds. *Tetrahedron* **1997**, *53*, 10123−10132.
(3) Reed, A. E.; Weinhold, F. Natural Bond Orbital Analysis of Internal Rotation Barriers and Related Phenomena. *Isr. J. Chem.* **1991**, *31*, 277−285 and references therein.
(4) Bader, R. F. W.; Cheeseman, J. R.; Laidig, K. E.; Wiberg, K. B.; Breneman, C. Origin of Rotation and Inversion Barriers. *J. Am. Chem. Soc.* **1990**, *112*, 6530−6536.
(5) Goodman, L.; Gu, H.; Pophristic, V. Flexing Analysis of Ethane Internal Rotation Energetics. *J. Chem. Phys.* **1999**, *110*, 4268−4275.
(6) Goodman, L.; Kundu, T.; Leszczynski, J. Getting the Shape of Methyl Internal Rotation Potential Surfaces Right. *J. Phys. Chem.* **1996**, *100*, 2770−2783 and references therein.
(7) Goodman, L.; Gu, H. Flexing Analysis of Steric Exchange Repulsion Accompanying Ethane Internal Rotation. *J. Chem. Phys.* **1998**, *109*, 72−78.
(8) Pophristic, V.; Goodman, L.; Guchhait, N. Role of Lone-Pairs in Internal Rotation Barriers. *J. Phys. Chem.* **1997**, *101*, 4290−4297.
(9) Goodman, L.; Pophristic, V. In *The Encyclopedia of Computational Chemistry*; Schleyer, P. v. R., Allinger, N. L., Clark, T., Gasteiger, J., Kollman, P. A., Schaefer, H. F., III, Schreiner, P. R., Eds.; John Wiley & Sons: Chichester, 1998; Vol. 4, pp 2525−2541.
(10) Ozkabak, A. G.; Goodman, L. Effect of Skeletal Relaxation on the Methyl Torsion Potential in Acetaldehyde. *J. Chem. Phys.* **1992**, *96*, 5958−5968.
(11) Mastryukov, V. S.; Samdal, S. Asymmetry in Methyl Group of Ethane During Internal Rotation: Ab Initio Study. *J. Comput. Chem.* **1998**, *19*, 1141−1145.
(12) Fukui, K. A Formulation of the Reaction Coordinate. *J. Phys. Chem.* **1970**, *74*, 4161−4163.
(13) Cioslowski, J.; Scott, A. P.; Radom, L. Catastrophes, Bifurcations and Hysteretic Loops in Torsional Potentials of Internal Rotation Molecules. *Mol. Phys.* **1997**, *91*, 413−420.
(14) Lister, D. G. *Introduction to Large Amplitude Motions in Molecules*; Academic Press: New York, 1978.
(15) E.g.: Kirtman, B.; Palke, W. E.; Ewig, C. S. Effect of Vibrations on the Internal Rotation Barrier in Ethane. *J. Chem. Phys.* **1976**, *64*, 1883−1890.
(16) Philis, J.; Berman, J. M.; Goodman, L. The Acetone a_2 Torsional Vibration. *Chem. Phys. Lett.* **1990**, *167*, 16−20.
(17) Lu, K.; Weinhlod, F.; Weisshaar, J. C. Understanding Barriers to Internal Rotation in Substituted Toluenes and Their Cations. *J. Chem. Phys.* **1995**, *102*, 6787−6805.
(18) Wiedmann, R. T.; Goodman, L.; White, M. Two-Color Zero Kinetic Energy-Pulsed Field Ionization Spectroscopy of the Acetone *n*-Radical Cation: the a_2 Torsional Vibration. *Chem. Phys. Lett.* **1998**, *293*, 391−396.
(19) Allen, L. C. Energy Component Analysis of Rotational Barriers. *Chem. Phys. Lett.* **1968**, *2*, 597−601.
(20) Brunck, T. K.; Weinhold, F. Quantum Mechanical Studies on the Origin of Barriers to Internal Rotation about Single Bonds. *J. Am. Chem. Soc.* **1979**, *101*, 1700−1709.
(21) Weisskopf, V. F. Of Atoms, Mountains, and Stars: A Study in Qualitative Physics. *Science* **1975**, *187*, 605−612.
(22) Badenhoop, J. K.; Weinhold, F. Natural Bond Orbital Analysis of Steric Interactions. *J. Chem. Phys.* **1997**, *107*, 5406−5421.
(23) Badenhoop, J. K.; Weinhold, F. Natural Steric Analysis of Internal Rotation Barriers. *Int. J. Quantum Chem.* **1999**, *72*, 269−280.

(24) Foster, J. P.; Weinhold, F. Natural Hybrid Orbitals. *J. Am. Chem. Soc.* **1980**, *102*, 7211−7218.
(25) Weinhold, F. In *The Encyclopedia of Computational Chemistry*; Schleyer, P. v. R., Allinger, N. L., Clark, T., Gasteiger, J., Kollman, P. A., Schaefer, H. F., III, Schreiner, P. R., Eds.; John Wiley & Sons: Chichester, 1998; pp 1792−1811.
(26) Pitzer, R. M. The Barrier to Internal Rotation in Ethane. *Acc. Chem. Res.* **1983**, *16*, 207−210.
(27) Mulliken, R. S. Intensities of Electronic Transition in Molecular Spectra. IV. Cyclic Dienes and Hyperconjugation. *J. Chem. Phys.* **1939**, *7*, 339−352.
(28) Senent, M. L.; Moule, D. C.; Smeyers, Y. G. An Ab Initio Determination of the Bending Torsion Torsion Spectrum of Dimethyl Ether, CH_3OCH_3 and CD_3OCD_3. *J. Chem. Phys.* **1995**, *102*, 5952−5959.
(29) Ozkabak, A. G.; Goodman, L. Skeletal Flexing During Methyl Rotation in Small Dimethyl Molecules. *Chem. Phys. Lett.* **1991**, *176*, 19−26.
(30) Pophristic, V. Mechanisms of Internal Rotation. Ph.D. Thesis, Rutgers University, New Brunswick, NJ, 1999.

AR990069F